Diagn Interv Radiol 2012; 18:11–19

ABDOMINAL IMAGING

ORIGINAL ARTICLE

Ideal combination of MRI sequences for perianal fistula classification and the evaluation of additional findings for readers with varying levels of experience

Nalan Yıldırım, Gökhan Gökalp, Ersin Öztürk, Abdullah Zorluoğlu, Tuncay Yılmazlar, İlker Ercan, Gürsel Savcı

PURPOSE

The aim of our study was to assess the contribution of various magnetic resonance imaging (MRI) sequences in determining the type of perianal fistula and in obtaining critical information for surgical decisions, as well as to define the optimal combination of sequences for readers with varying levels of experience.

MATERIALS AND METHODS

The study included 33 MRI examinations in 26 patients with suspected perianal fistula. The following sequences were obtained in both the coronal and axial planes: thin slice, high resolution T1-weighted (W) spin echo; T2-weighted turbo spin echo; short tau inversion recovery (STIR); and native and contrast enhanced T1-weighted gradient echo fast low-angle shot (FLASH) images with fat suppression (FS-CE-T1W-GRE). The examinations were interpreted by three radiologists with varying degrees of experience in two different sessions, and the inter-reader agreement was assessed. Seventeen of the patients underwent surgery. The agreement between the surgical findings and the MRI results were evaluated.

RESULTS

A statistically significant concordance between the fistula classification and surgery was achieved with the FS-CE-T1W-GRE sequence for Reader 1 (Cramer's V=0.701, P = 0,022) and Reader 3 (Cramer's V=0.716, P = 0,043). For Reader 2, statistically significant concordance between fistula classification and surgery was achieved with the FS-CE-T1W-GRE (Cramer's V=0.703, P = 0,011) and the T2W images (Cramer's V=0.648, P = 0,027). For all sequences, there was statistically significant agreement between readers for fistula classification, internal opening location, and the presence of sinus tracts, abscess, a horseshoe component, and inflammation.

CONCLUSION

For experienced readers, combining FS-CE-T1W-GRE images with either T2W or STIR images collected in both the coronal and axial planes was sufficient to make an assessment before deciding the surgical extent of the procedure.

Key words: • *rectal fistula* • *magnetic resonance imaging*

From the Departments of Radiology (N.Y. ✉ *nalanmed76@hotmail.com*, G.G., G.S.), General Surgery (E.Ö., A.Z., T.Y.), and Biostatistics (İ.E.), Uludağ University School of Medicine, Bursa, Turkey.

Received 25 November 2010; revision requested 5 January 2011; revision received 10 January 2011; accepted 12 January 2011.

Published online 23 February 2011
DOI 10.4261/1305-3825.DIR.4092-10.1

Perianal fistula is a common disease that most commonly originates from anal gland infections. Medical therapy has little treatment value, and patients eventually undergo surgery. The success of the surgery is closely associated with the preoperative evaluation (1). Therefore, it is of utmost importance to evaluate the course of the fistula and the presence of associated findings before surgical intervention because it can influence the surgical approach (2). Also, because recurrence is one of the most important problems following surgery, identification of the extensions of the disease with imaging methods aids in the surgical elimination of all sources of infection and ultimately decreases the percentage of recurrent disease (3).

The preoperative evaluation of a fistula track by a surgeon includes inspection, palpation, probing, and the injection of colored dyes (2). The imaging methods employed to evaluate perianal fistulas are fistulography, computed tomography (CT), three dimensional (3D) endoanal ultrasonography (EAUS) (with or without the instillation of hydrogen peroxide into the track), and magnetic resonance imaging (MRI) with endoanal or pelvic coils or both. The description and classification of the primary track, the location of the internal opening (the radial site and the level), the presence of extensions (especially horseshoe extensions) and the presence of an abscess formation are the critical parameters for a complete evaluation of a fistula and should be implicated in the radiological reports. MRI is reported to be the most sensitive imaging method because it allows for the evaluation of secondary tracks and the detection of any possible extension to the supralevator fossa. Previous investigations performed to determine the role of MRI in this problem have indicated the value of the technique (2, 4–11). A concordance rate of 86%–88% between MRI and surgical findings was reported for the detection and classification of fistulas (12, 13).

To the best of our knowledge, no previous reports have evaluated the value of each sequence for assessing the specific surgical parameters in addition to fistula classification. The purpose of our study was to assess the contribution of different MRI sequences in determining the perianal fistula type and in obtaining critical information for surgical decisions, as well as to define the optimal combination of sequences for readers with varying levels of experience.

Materials and methods

Patient selection

Thirty-three MRI examinations in 26 patients, obtained between 2007 and 2010, were included in the study. Fifteen of the patients were male, and 11 were female. The ages of the patients ranged from 30 to 84 years (mean age, 48 years). Three patients were known to have underlying inflammatory bowel disease. There was no evidence of diabetes melli-

tus in any of the patients. Seventeen of the 33 patients underwent surgery following their MRI examination (fistulectomy, seton placement). The MRI was performed between 1 and 22 days prior to the surgery (mean interval, 7 days). Institutional review board approval was obtained. Because our study was retrospective, no informed consent was obtained.

MRI

The MRI protocols for all of the cases were standard. The images were obtained with a 1.5 T MR scanner (Magnetom Vision, Siemens, Erlangen, Germany). The patient was placed in a supine position, and a phased-array coil was used for image acquisition. Half-Fourier acquisition turbo spin echo (HASTE) axial and sagittal images were used as localizers for the subsequent sequences. Distal rectum and subcutaneous tissue were included in the imaging volume. The acquisition was planned so that the imaging plane included the supralevator space to ensure that no extensions were present. An oblique coronal image was obtained parallel to the anal canal, and an axial image was obtained perpendicular to the coronal plane.

The sequence of the parameters was as follows:

1. T1-weighted (T1W) axial and coronal spin echo (TR/TE, 680–700/14 ms; field of view [FOV], 20–23 cm; matrix size, 512×245; acquisition, 1; slice thickness, 4 mm; gap, 0.4 mm)
2. T2-weighted (T2W) turbo spin echo axial and coronal (TR/TE, 4000/130 ms; FOV, 23 cm; matrix size, 512×512; slice thickness, 4 mm; gap, 0.4 mm)
3. Short tau inversion recovery (STIR) axial and coronal (TR/TE, 4000/30 ms; TI, 150; FOV, 16 cm; matrix size, 256×512; slice thickness, 5 mm; gap, 0.6 mm); and
4. T1W gradient echo (fast low-angle shot, FLASH) native and contrast-enhanced axial and coronal images with fat suppression (TR/TE, 160/4 ms; FOV, 23 cm; flip angle 80°; matrix, 256×512; slice thickness, 5 mm; gap, 0.5 mm); the standard dose of 0.1 mmol/kg of gadopentetate dimeglumine was injected.

Image analysis

MR images were retrospectively interpreted by two experienced radiologists who primarily worked with abdominal imaging, and after a training session, one experienced general radiologist without any experience with perianal fistula imaging. Two of the radiologists were kept blind to the clinical data, and each MRI sequence was evaluated individually in separate sessions in a mixed fashion; there were 2–3 days between all sessions. The other radiologist was involved in the clinical care of the patients and routinely reported the MRI examinations but was blinded to the clinical or surgical results at the time of the review.

The aim of MR imaging was to answer the critical surgical questions prior to the surgical intervention. These questions concerned the type of the fistula (according to the Parks classification), the location of the internal opening, presence or absence of any abscess formation, determination of any possible secondary tracks, detection of possible supralevator extension and the distance between the internal opening and the anal verge (14).

Fistula type was noted according to the following classification: intersphincteric, trans-sphincteric, suprasphincteric, extrasphincteric, submucosal, no fistula or uncertain. The location of the internal opening with respect to a clock face (1–12), the presence or absence of sinus tracks, abscesses, a horseshoe component and coexisting inflammation and the distance of the internal opening to the anal orifice (in mm) were noted for each of the MRI sequences listed above. It was also noted if no decision could be made.

Either the continuation of the primary tract itself into the anal mucosa or the radial site closest to the maximal inflammation found in the intersphincteric space was accepted as the internal opening. The internal opening was described with respect to a clock face, with 12-o'clock being anterior. The patients were in a supine position during image acquisition and the surgical and imaging positions of the patients were identical.

Surgical evaluation

The type of the fistula according to Parks classification was noted by a surgeon who was unaware of the MRI findings. The internal opening was noted after inspection of the anal lumen during instillation of methylene blue via the external opening of the track. The presence or absence of sinus tracks, abscess formations, a horseshoe component, inflammation and the distance of the internal opening to the anal orifice (in mm) were also noted during the surgery.

Statistical analysis

A commercially available software package (Statistical Package for Social Sciences, version 11.0, SPSS Inc., Chicago, Illinois, USA) was used for all statistical analyses. A P value of less than 0.05 was considered to indicate a statistically significant difference. The agreement between the surgical evaluation and Readers 1, 2 and 3 was evaluated separately using Cramer's V coefficient.

The inter-reader agreement for fistula classification, internal opening with respect to a clock-face and the presence of sinus tracts, abscess, a horseshoe component and inflammation was evaluated with Cramer's V coefficient. The inter-reader agreement for the distance between the anal opening and the internal opening of the fistula track was evaluated using intra-class correlation coefficients.

Results

Thirty-three MRI studies in 26 consecutive patients were assessed for interobserver agreement. The parameters were evaluated separately for each sequence. Seventeen of these patients underwent surgery. The surgical classification of the fistulas was as follows: intersphincteric (n=3, 17%), transsphincteric (n=9, 53%), superficial-submucosal (n=2, 12%), and extrasphincteric (n=1, 6%). No fistula was detected in two patients (12%). The internal openings of these fistulas were located at the following clock-face positions: 6 (n=8), 5 (n=1), 11 (n=3), and 7 (n=2). The internal opening was not detected in three patients. Sinus tracks were detected in all but two patients (88%). In one patient, no note concerning sinus tracks was taken during surgery. Abscesses were identified in two patients (12%). A horseshoe component was found in three patients (18%). Inflammation was detected in ten of the seventeen patients (59%).

The agreement between the surgical findings and each reader's evaluation is illustrated in Table 1. For Reader 1, a statistically significant concordance between fistula classifications and surgical findings was achieved with

the FS-CE-T1W-GRE images (Cramer's V=0.701, P = 0.022). Agreement between the MR images and the surgical findings for internal opening location was found for the FS-CE-T1W-GRE and T2W images (Cramer's V=0.869, P = 0.001 and Cramer's V=0.805, P = 0.001, respectively). The highest concordance with sinus track presence was obtained from the T2W and STIR sequences (Cramer's V=0.739, P = 0.001 and Cramer's V=0.681, P = 0.005, respectively). Detection of abscess formation was best correlated with surgery for the T2W (Cramer's V=0.789, P = 0.001) images. The presence or absence of a horseshoe extension was best correlated with surgery for the FS-CE-T1W-GRE (Cramer's V=0.784, P = 0.002) and T1W (Cramer's V=0.784, P = 0.010) images. A statistically significant correlation with inflammation was detected for the FS-CE-T1W-GRE images (Cramer's V=0.764, P = 0.013). No significant correlation was found between surgical and MRI results for the anal verge/internal opening distance.

For Reader 2, a statistically significant concordance between fistula classification and the surgical findings was achieved with the FS-CE-T1W-GRE (Cramer's V=0.703, P = 0.011) and T2W (Cramer's V=0.648, P = 0.027) images. Agreement between the MR images and surgical findings for internal opening location was found for the T2W (Cramer's V=0.920, P < 0.001), FS-CE-T1W-GRE (Cramer's V=0.879, P < 0.001) and STIR images (Cramer's V=0.803, P = 0.016). Statistically significant concordance with sinus track presence was obtained for the STIR sequences (Cramer's V=0.856, P < 0.001). Detection of abscess was significantly correlated with surgery for all sequences (Cramer's V=1.000, P < 0.001). The presence or absence of a horseshoe extension was best correlated with the surgical findings for the FS-CE-T1W-GRE (Cramer's V=1.000, P < 0.001) and T1W (Cramer's V=1.000, P < 0.001) images. A statistically significant correlation with inflammation was detected for the T1W (Cramer's V=0.873, P = 0.003), FS-CE-T1W-GRE (Cramer's V=0.770, P = 0.009) and T2W (Cramer's V=0.759, P = 0.007) images. No significant correlation was found between the surgical and MRI results for anal orifice-internal opening distance for Reader 2.

Table 1. Agreement between the surgical results and the assessed parameters for Readers 1, 2, and 3

		T1W		T2W		STIR		T1W GRE -/+ Gd	
Readers	Parameters	Cramer's V	*P*	Cramer's V	*P*	Cramer's V	*P*	Cramer's V	*P*
Reader 1	Parks classification	-	0.514	0.534	0.266	0.594	0.152	0.701	0.022
	Internal opening	0.575	0.706	0.805	0.001	0.573	0.396	0.869	0.001
	Sinus tract	0.395	0.32	0.739	0.001	0.681	0.005	0.491	0.124
	Abscess	NP	NP	0.789	0.001	0.537	0.099	NP	NP
	Horseshoe	0.784	0.01	0.595	0.014	0.561	0.081	0.784	0.002
	Inflammation	0.436	0.241	0.425	0.216	0.545	0.93	0.764	0.013
	Distance	-	0.754	-	0.568	-	0.456	-	0.628
Reader 2	Parks classification	0.566	0.256	0.648	0.027	0.605	0.13	0.703	0.011
	Internal opening	0.811	0.074	0.92	<0.001	0.803	0.016	0.879	<0.001
	Sinus tract	0.3	0.611	0.508	0.067	0.856	<0.001	0.495	0.097
	Abscess	1	<0.001	1.000	<0.001	1.000	<0.001	1.000	<0.001
	Horseshoe	1	<0.001	0.854	0.002	0.787	0.007	1.000	<0.001
	Inflammation	0.873	0.003	0.759	0.007	0.429	0.086	0.77	0.009
	Distance	-	0.762	-	0.558	-	0.537	-	0.681
Reader 3	Parks classification	-	0.544	-	0.051	-	0.363	0.716	0.043
	Internal opening	-	0.073	0.866	0.001	-	0.102	0.904	0.005
	Sinus tract	-	0.32	0.739	0.001	0.681	0.005	-	0.124
	Abscess	NP	NP	-	0.697	0.531	0.047	-	0.806
	Horseshoe	-	0.236	0.786	0.010	0.679	0.011	0.784	0.014
	Inflammation	-	0.747	-	0.3	-	0.533	-	0.394
	Distance	-	0.681	-	0.558	-	0.762	-	0.491

Agreement between surgery and parameters other than distance was evaluated using Cramer's V coefficient. Agreement between the distance assessment and surgery was evaluated using intraclass correlation coefficients.
NP, statistical analysis is not possible.

Figure 1. a, b. A female patient under follow-up for Crohn's disease who presented with several external openings in the perianal region. T2W TSE coronal MR images **(a)** of the perianal region reveal the fistula track *(arrow)* filled with pus within the perianal fat tissue on the right side. The track also has a horseshoe component (not shown), and on the left side, its supralevator component *(arrowhead)* is in close proximity to the inflamed sigmoid colon *(hollow triangle)*. Contrast enhanced T1-weighted GRE coronal images **(b)** indicate the enhanced, inflamed bowel segment *(hollow triangle)* and the supralevator component of the fistula *(arrow)*. No abscess was detected. The inter-reader agreement was excellent for all parameters.

For Reader 3, a statistically significant concordance between fistula classification and surgery was achieved with the FS-CE-T1W-GRE images (Cramer's V=0.716, P = 0.043). Agreement between the MR images and surgical findings for internal opening location was found for the T2W (Cramer's V=0.866, P = 0.001) and FS-CE-T1W-GRE (Cramer's V=0.904, P = 0.005) images. A statistically significant concordance between sinus track presence was obtained with the T2W (Cramer's V=0.739, P = 0.001) and STIR (Cramer's V=0.681, P = 0.005) sequences. The detection of abscess was best correlated with the surgical findings for the STIR images (Cramer's V=0.531, P = 0.047). The presence or absence of a horseshoe extension was significantly correlated with the surgical findings for the FS-CE-T1W-GRE (Cramer's V=0.784, P = 0.014), T2W (Cramer's V=0.786, P = 0.010) and STIR (Cramer's V= 0.679, P = 0.011) images. No statistically significant correlation between surgical findings and MRI results was detected with any of the sequences for inflammation or distance.

According to these results, the FS-CE-T1W-GRE sequence provided the highest concordance with the Parks classification of fistulas for all readers. The sequences in agreement with the surgical results for the other parameters showed variability between the readers. The highest concordance among all the parameters was reached with the combination of the T2W and FS-CE-T1W-GRE sequences for Reader 1. For Reader 2, the addition of the STIR or T2W sequences to the FS-CE-T1W-GRE images provided the highest agreement. For Reader 3, the T2W and FS-CE-T1W-GRE sequences and the STIR images offered similar performance.

The inter-reader agreement was evaluated for the 33 MRI examinations. For all of the sequences, there was a statistically significant agreement between readers for fistula classification and internal opening location, as well as the presence of sinus tracts, abscess, a horseshoe component and inflammation. The highest concordance was for inflammation using the STIR sequence (Cramer's V=1.000, P < 0.001) and for abscess using the FS-CE-T1W-GRE images (Cramer's V=1.000, P < 0.001). The lowest concordance was for sinus tracts using the STIR sequence (Cramer's V=0.612, P < 0.001). Findings in the various sequences are illustrated in Figs. 1–3.

The inter-reader agreement for the distance between the anal opening and the internal opening of the primary fistula tract was evaluated using intraclass correlation coefficients. There was no agreement for the T1W, T2W or STIR sequences, while a statistically significant agreement was found for the FS-CE-T1W-GRE sequence (r=0.648, P = 0.001).

Discussion

Perianal fistulas affect nearly 10 in 100 000 of the general population (15). The disease predominantly strikes young adults, and men are more commonly affected (3). Perianal fistulas occur either as a component of inflammatory bowel disease, such as Crohn's disease, or as a consequence of localized infection of the anal crypts and glands, cryptoglandular disease (16, 17). Trauma, infection, and iatrogenic causes are less commonly encountered etiological factors in the disease (17).

The surgical treatment for this disorder involves incision of the fistula track over a metal probe placed into the track (fistulotomy or fistulectomy), seton placement and more complex techniques (15). The primary objective of the treatment is to eradicate the infection while preserving anal continence (3). To achieve this goal, the surgeon needs to know the relationship of the tract to the anal sphincter muscles and the presence and location of all of

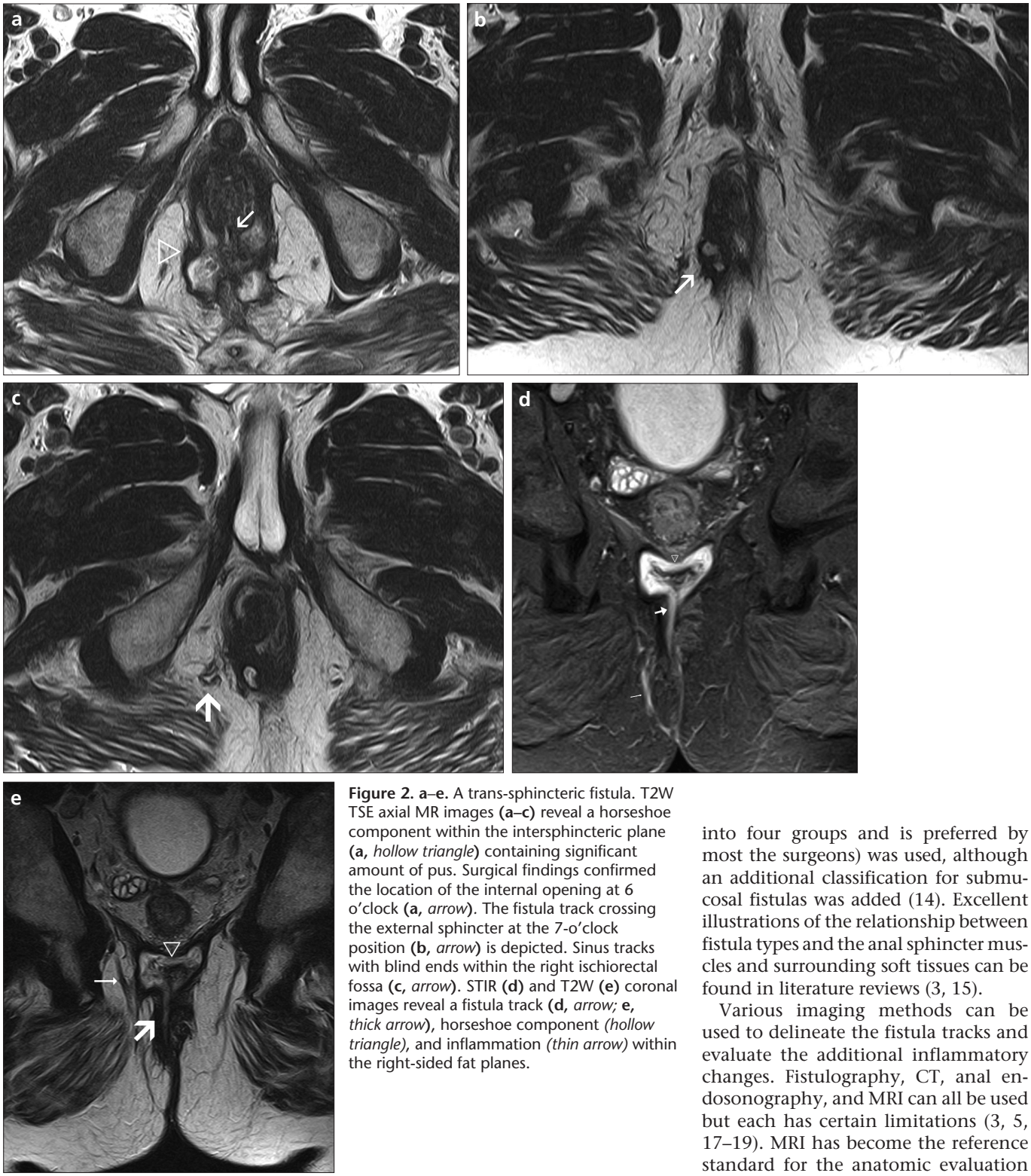

Figure 2. a–e. A trans-sphincteric fistula. T2W TSE axial MR images **(a–c)** reveal a horseshoe component within the intersphincteric plane **(a,** *hollow triangle***)** containing significant amount of pus. Surgical findings confirmed the location of the internal opening at 6 o'clock **(a,** *arrow***)**. The fistula track crossing the external sphincter at the 7-o'clock position **(b,** *arrow***)** is depicted. Sinus tracks with blind ends within the right ischiorectal fossa **(c,** *arrow***)**. STIR **(d)** and T2W **(e)** coronal images reveal a fistula track **(d,** *arrow;* **e,** *thick arrow***)**, horseshoe component *(hollow triangle)*, and inflammation *(thin arrow)* within the right-sided fat planes.

the extensions that could lead to recurrence if not properly treated (3).

At present, two classifications are most commonly used: a classification proposed by Parks in 1976, which was created for surgical use, and the St James University Hospital classification, which was developed based on a MRI examination (Tables 2 and 3) (14, 15). The anatomic course of a fistula between the internal enteric opening and the perianal skin determines the class of the fistula (3). In our study, the Parks classification (which classifies fistulas into four groups and is preferred by most the surgeons) was used, although an additional classification for submucosal fistulas was added (14). Excellent illustrations of the relationship between fistula types and the anal sphincter muscles and surrounding soft tissues can be found in literature reviews (3, 15).

Various imaging methods can be used to delineate the fistula tracks and evaluate the additional inflammatory changes. Fistulography, CT, anal endosonography, and MRI can all be used but each has certain limitations (3, 5, 17–19). MRI has become the reference standard for the anatomic evaluation of perianal and ano- or rectovaginal fistulas (20). Body coils, pelvic phased array coils and endoanal coils can be used to image and classify fistulas (17). Currently, MRI examinations are performed with endoanal coils, phased array coils or with the combination of two, which provides complementary benefits (17).

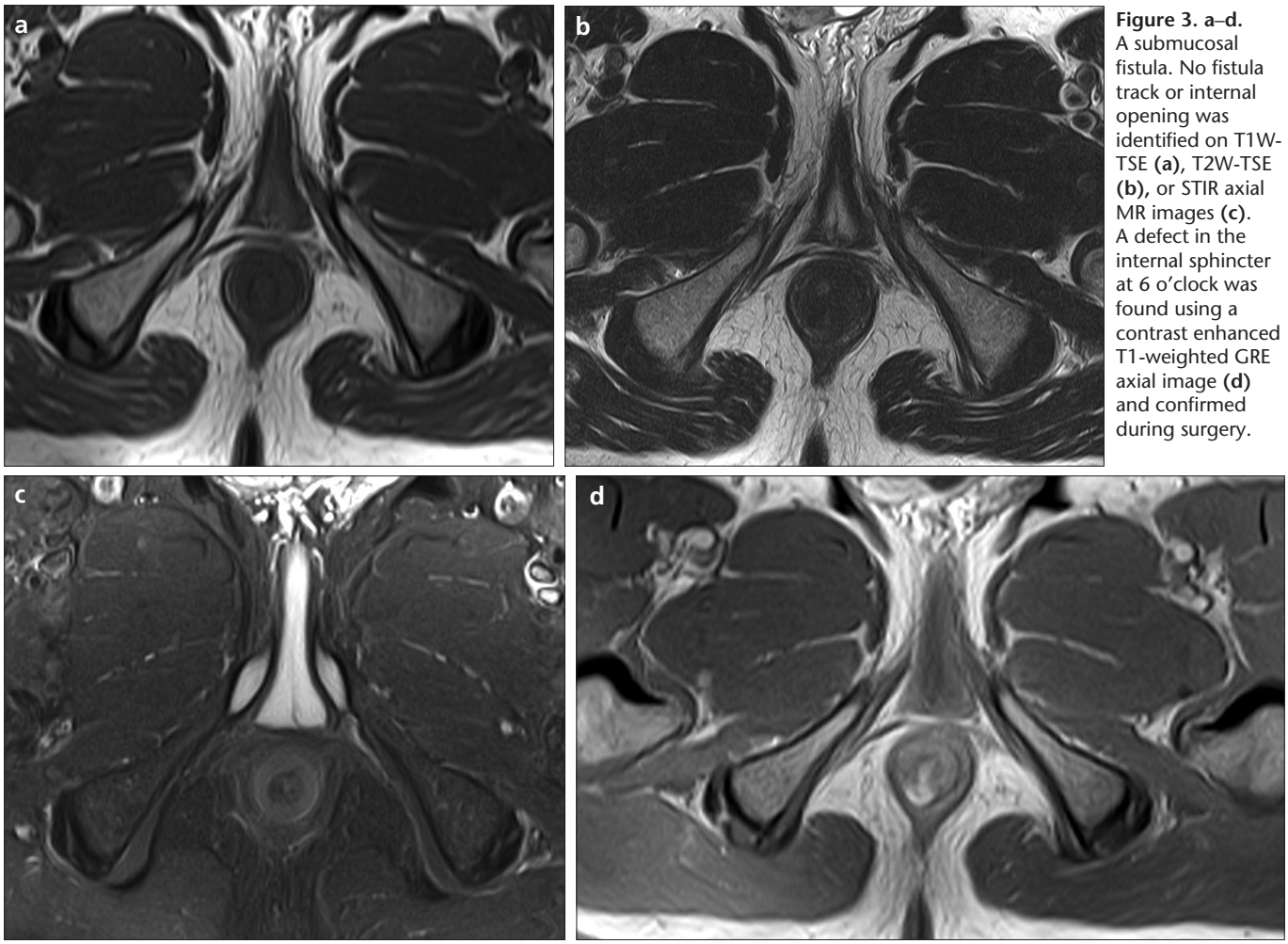

Figure 3. a–d. A submucosal fistula. No fistula track or internal opening was identified on T1W-TSE **(a)**, T2W-TSE **(b)**, or STIR axial MR images **(c)**. A defect in the internal sphincter at 6 o'clock was found using a contrast enhanced T1-weighted GRE axial image **(d)** and confirmed during surgery.

Table 2. Parks classification of perianal fistula (17)

Fistula type	Description
Intersphincteric	Confined to intersphincteric plane, does not cross external sphincter or levator muscles
Trans-sphincteric	Track passes radially through external sphincter
Suprasphincteric	Track passes upward within intersphincteric plane over puborectalis muscles and descends through levator muscles, ischiorectal fossa
Extrasphincteric	Fistula's course is completely outside external sphincter

Table 3. St. James's University Hospital MRI classification system (14)

Grade	Description
0	Normal appearance
1	Simple linear intersphincteric fistula
2	Intersphincteric fistula with intersphincteric abscess or secondary fistulous track
3	Trans-sphincteric fistula
4	Trans-sphincteric fistula with abscess or secondary track within the ischioanal or ischiorectal fossa
5	Supralevator and translevator disease

MRI may include various sequences and additional techniques. It is possible to visualize the whole sphincter complex and the track itself (18). Images obtained in the coronal plane particularly aid surgery by indicating the relationship of the fistula to the levator ani and puborectalis muscles (5). There are a limited number of studies in the literature that specifically address the value of MRI sequences in perianal fistula imaging (2, 4, 5–7, 13).

It is known that T2W images enable discrimination between the fibrous and pus-filled portions of the tracks, and visualization of the muscle layers forming the anal sphincter (3). T1W sequences are usually combined with contrast enhanced sequences (3). Fat-suppression techniques can be added to both sequences, and the STIR sequence also can be used (3). STIR sequences provide good fat suppression and inflammation is easily depicted due to the long T1 and T2 relaxation times (5). In our study, the STIR sequence results were well-correlated with the surgical findings for sinus track, abscess, internal opening and horseshoe extension evaluation. By contrast, there was no significant correlation for inflammation. This finding is probably due to the fact that MRI is able to detect inflammation with greater sensitivity, whereas inflammation is not a straightforward assessment during surgery. T1W sequences with fat saturation after intravenous gadolinium administration also help in detecting the tracks that are less conspicuous on T2W sequences (17). In our study, the FS-CE-T1W-GRE images showed statistically significant agreement between the fistula classification results from surgery and MRI interpretation for Readers 1 and 3. For Reader 2, the FS-CE-T1W-GRE and T2W images were in agreement with the surgical findings. These findings are consistent with the results of Spencer et al. (6), who suggested that axial and coronal contrast-enhanced T1W and axial T2W sequences should provide adequate information to guide surgery. In our study, however, we evaluated a more detailed classification of fistulas and internal openings, the positions of which were indicated by reference to a clock face (1–12). Also, additional findings, such as the presence of a horseshoe extension or inflammation, were evaluated separately.

Two trans-sphincteric fistulas were misclassified as intersphincteric fistulas by both readers based on the FS-CE-T1W-GRE images. When the images were retrospectively evaluated, it was apparent that the intersphincteric component of the fistula tract was clearly depicted, whereas the tract passed far below the external sphincter; as a result, it was hard to decide if the tract really passed the sphincter or lay completely within the intersphincteric space. Also, in two cases, both readers and the surgical evaluation were unable to demonstrate any fistula tracts, and the clinical follow-up was unremarkable.

The internal opening was successfully depicted by Readers 1 and 3 using FS-CE-T1W-GRE and T2W images. For Reader 2, the T2W, FS-CE-T1W-GRE and STIR images (in decreasing order of significance) were statistically in agreement with the surgical findings.

In three patients, no internal opening was found during surgery. These patients had no complaints after the procedure. In one patient, no internal opening was found in two previous operations, despite MR reports that mentioned an opening at the 6-o'clock position (these reports were not included in our study). This opening was correctly identified at the third MRI examination (which was included in our study) by all of the readers and was also found during the third surgery (Fig. 4).

Fistulas may contain an isolated track (patent or fibrotic-simple) or may have additional parts, such as secondary tracks, interconnecting ramifications, a horseshoe configuration or abscesses that result in a complex form (3, 18). It is called a 'horseshoe' if the extension occurs in the horizontal plane (3). In complex fistulas, it has been shown that MRI is more successful at showing secondary tracks than both examination and surgery (18). We demonstrated that the T2W (Readers 1 and 3) and STIR (Readers 1, 2 and 3) images successfully indicated the sinus tracts. Abscesses were identified using the T2W images (Reader 1), STIR images (Reader 3) and all of the sequences (Reader 2). For Reader 1, the surgical findings were statistically in agreement with the horseshoe component demonstration using the FS-CE-T1W-GRE, T1W and T2W images. For Reader 2, all of the sequences were in agreement with the surgical findings for showing a horseshoe component, whereas Reader 3 achieved concordant results with surgery using the T2W, STIR and FS-CE-T1W-GRE sequences.

MRI of the perianal region can provide detailed information about perianal disease activity in chronic inflammatory bowel disease and related anal disorders. Horsthuis et al. (11) showed that dynamic contrast enhanced MRI can provide both anatomical and functional information on disease activity and could be used to identify the subpopulation of patients who should be monitored more closely due to the risk of extensive disease progression. In our study, inflammation was most accurately indicated by the FS-CE-T1W-GRE images for Reader 1 and Reader 2, whereas statistically significant agreement was achieved for Reader 2 using the T1W and T2W sequences as well. There were no statistically significant agreements between surgery and the imaging results for Reader 3.

For all of the readers, there was no statistically significant agreement between the surgical and imaging results for the distance between the internal opening and anal verge. This finding may be due to the varying experiences of the readers and an inadequate consensus between the observers before the measurements. The STIR images may be helpful to inexperienced observers for the detection of the fistula and for definition of its course. Also, surgical measurement may be less precise, and structures may change configuration and length during instrumentation.

Direct injection of the fistulas with water or gadopentetate dimeglumine has been shown to improve their delineation (2, 21), although this technique cannot be performed on tracks that do not have an external opening (18). Sabir et al. (22) have described an approach using rectal Gd-DTPA. Ergen et al. (23) have also demonstrated the usefulness of rectal contrast material administration and subsequent forceful defecation to depict rectovaginal or anovaginal fistula openings inside the rectum. Digital subtraction MR fistulography has been described by Schaefer et al. (24). These techniques all lengthen the time needed and increase the complexity required to collect the images, which may be a problem in busy departments. As each day passes, it becomes more critical to complete imaging within a reasonable

Figure 4. a–e. A trans-sphincteric fistula. The patient had two previous operations for perianal fistula. The internal opening was not detected preoperatively, despite an opening at the 6-o'clock position being detected in the preoperative MRI. Another MRI was performed due to ongoing complaints by the patient. The fistula was indicated, and the patient has been symptom free since surgery. A STIR axial MR image **(a)** of the anal canal indicates the correctly predicted internal opening at 6 o'clock *(arrow).* A T2W TSE axial image **(b)** reveals the fistula track traversing the external sphincter on the right side *(arrowhead).* The external sphincter *(thin arrow)* and the fibrous tissue surrounding the track *(hallow triangle)* are seen. A caudal section of Panel B **(c)**, indicating the distal portion of the fistula track coursing within the fat tissue after traversing the external sphincter *(arrow)*. A contrast enhanced T1W gradient echo fat suppressed axial image **(d)** clearly demonstrates the enhanced internal sphincter *(asterisk),* the intersphincteric plane, and the internal opening *(arrow)*. A STIR axial image **(e)** of the fistula track and the linear sinus tracks lying posteriorly *(arrow)*.

time period. Recently, Hori et al. (25) evaluated the usefulness of diffusion weighted MRI in combination with fat suppressed T2W imaging compared to gadolinium enhanced MRI with T2W images. They indicated that some fistula tracks can be shown with higher confidence and sensitivity using additional diffusion weighted images but that the additional value was similar to that achieved by gadolinium enhanced images (25). They only evaluated the

presence or absence of a fistula and the extent of the tracks and did not comment on other parameters (such as the internal opening, abscess and presence of a horseshoe component) that are important for patient care, however.

There are some limitations to our study. Even though surgical findings have been accepted as the reference standard, it is known that surgery may miss some fistulae and accompanying pathologies. Therefore, surgery may not offer a reliable "reference standard" for perianal fistula disease. Long-term follow-up results also would be helpful for evaluating the MRI examination findings.

In addition, this was a retrospective study with a limited number of patients who mostly presented intersphincteric and trans-sphincteric fistulae. Also, new MRI techniques enabling volumetric imaging with isotropic resolution will undoubtedly be of great use for perianal fistula imaging. These innovations will add to fistula imaging by allowing higher quality images with 3D reconstruction capabilities and shorter imaging times due to the need for only axial images.

Patients definitely benefit from a detailed preoperative examination that provides a clear map for the surgeon. MRI is the method that is usually employed, particularly in patients with Crohn's disease. It is sometimes a problem to keep a patient in an MRI suite for extended periods of time. In such circumstances, or in busy departments, it is still possible to obtain adequate information by combining certain sequences.

In conclusion, our results indicate that high resolution MRI of perianal fistula disease is in good agreement with surgery and has low interobserver variance. For experienced readers, combining FS-CE-T1W-GRE images with either T2W or STIR images in both the coronal and axial planes was sufficient to obtain answers to the surgeon's questions before deciding the extent of the surgical procedure. Readers who are experienced in other areas but do not routinely work with the perianal region imaging may need and benefit from all sequences (except T1W) equally.

Conflict of interest disclosure

The authors declared no conflicts of interest.

References

1. Michalopoulos A, Papadopoulos V, Tziris N, Apostolidis S. Perianal fistulas. Tech Coloproctol 2010; 14 Suppl 1:S15–17.
2. Myhr GE, Myrvold HE, Nilsen G, Thoresen JE, Rinck PA. Perianal fistulas: use of MR imaging for diagnosis. Radiology 1994; 191:545–549.
3. Halligan S, Stoker J. Imaging of fistula in ano. Radiology 2006; 239:18–33.
4. Koelbel G, Schmiedl U, Majer MC, et al. Diagnosis of fistulae and sinus tracts in patients with Crohn disease: value of MR imaging. Am J Roentgenol 1989; 152:999–1003.
5. Haggett PJ, Moore NR, Shearman JD, et al. Pelvic and perineal complications of Crohn's disease: assessment using magnetic resonance imaging. Gout 1995; 36:407–410.
6. Spencer JA, Ward J, Beckingham IJ, Adams C, Ambrose NS. Dynamic contrast-enhanced MR imaging of perianal fistulas. AJR Am J Roentgenol 1996; 167:735–741.
7. Halligan S, Healy JC, Bartram CI. Magnetic resonance imaging of fistula-in-ano: STIR or SPIR? Br J Radiol 1998; 842:141–145.
8. Spencer JA, Chapple K, Wilson D, et al. Outcome after surgery for perianal fistula: predictive value of MR imaging. AJR Am J Roentgenol 1998; 171:403–406.
9. Beets-Tan RG, Beets GL, van der Hoop AG, et al. Preoperative MR imaging of anal fistulas: does it really help the surgeon? Radiology 2001; 218:75–84.
10. Buchanan GN, Halligan S, Bartram CI, et al. Clinical examination, endosonography, and MR imaging in preoperative assessment of fistula in ano: comparison with outcome-based reference standard. Radiology 2004; 233:674–681.
11. Horsthuis K, Lavini C, Bipat S, Stokkers PCF, Stoker J. Perianal Crohn disease: evaluation of dynamic contrast enhanced MR imaging as an indicator of disease activity. Radiology 2009; 251:380–387.
12. Lunniss PJ, Armstrong P, Barker PG, Reznek RH, Phillips RK. Magnetic resonance imaging of anal fistulae. Lancet 1992; 340:394–396.
13. Barker PG, Lunniss PJ, Armstrong P, Reznek RH, Cottam K, Phillips RK. Magnetic resonance imaging of fistula-in-ano: technique, interpretation and accuracy. Clin Radiol 1994; 49:7–13.
14. Morris J, Spencer JA, Ambrose NS. MR imaging classification of perianal fistulas and its implications for patient management. Radiographics 2000; 20:623–635.
15. Hussain SM, Outwater EK, Joekes EC, et al. Clinical and MR imaging features of cryptoglandular and Crohn's fistulas and abscesses. Abdom Imaging 2000; 25:67–74.
16. Sun MR, Smith MP, Kane RA. Current techniques in imaging of fistula in ano: three-dimensional endoanal ultrasound and magnetic resonance imaging. Semin Ultrasound CT MR 2008; 29:454–471.
17. Parks AG, Gordon PH, Hardcastle JD. A classification of fistula-in-ano. Br J Surg 1976; 63:1–12.
18. Stoker J, Rociu E, Wiersma TG, Laméris JS. Imaging of anorectal disease. Br J Surg 2000; 87:10–27.
19. Kruskal JB, Kane RA, Morrin MM. Peroxide-enhanced anal endosonography: technique, image interpretation, and clinical applications. Radiographics. 2001; 21:173–189.
20. Sahni VA, Ahmad R, Burling D. Which method is best for imaging of perianal fistula? Abdom Imaging 2008; 33:26–30.
21. Algra PR. Gadopentate dimeglumine-enhanced MR imaging of spinal dermal sinus tract. AJNR 1991; 12:1025–1026.
22. Sabir N, Sungurtekin U, Erdem E, Nessar M. Magnetic resonance imaging with rectal Gd-DTPA: new tool for the diagnosis of perianal fistula. Int J Colorectal Disease 2000; 15:317–322.
23. Ergen FB, Arslan EB, Kerimoglu U, Akata D. Magnetic resonance fistulography for the demonstration of anovaginal fistula: an alternative imaging technique? J Comput Assist Tomogr 2007; 31:243–246.
24. Schaefer O, Lohrmann C, Langer M. Assessment of anal fistulas with high-resolution subtraction MR-fistulography: comparison with surgical findings. J Magn Reson Imaging 2004; 19:91–98.
25. Hori M, Oto A, Orrin S, Suzuki K, Baron RL. Diffusion-weighted MRI: a new tool for the diagnosis of fistula in ano. J Magn Reson Imaging 2009; 30:1021–1026.